Swin Transformer: Hierarchical Vision Transformer using Shifted Windows

Ze Liu, Yutong Lin, Yue Cao, Han Hu et al.

Microsoft Research Asia

ICCV 2021 Best Paper Award

Presented by Minho Park

Contribution

- **Propose Swin Transformer:** A hierarchical Transformer whose representation is computed with ***S****hifted* ***win****dows*.
- **Use stage structure (for FPN).**
- Ablation studies include **relative positional encoding.**

Shifted Window Approach

- CNN (VGG, ResNet, etc.)
- Global attention (ViTs)
- Local attention (Sliding Window, Axial attention, Swin)

$$\Omega(\mathrm{MSA}) = 4hwC^2 + 2(hw)^2C, \quad (1)$$

$$\Omega(\text{W-MSA}) = 4hwC^2 + 2M^2hwC, \quad (2)$$

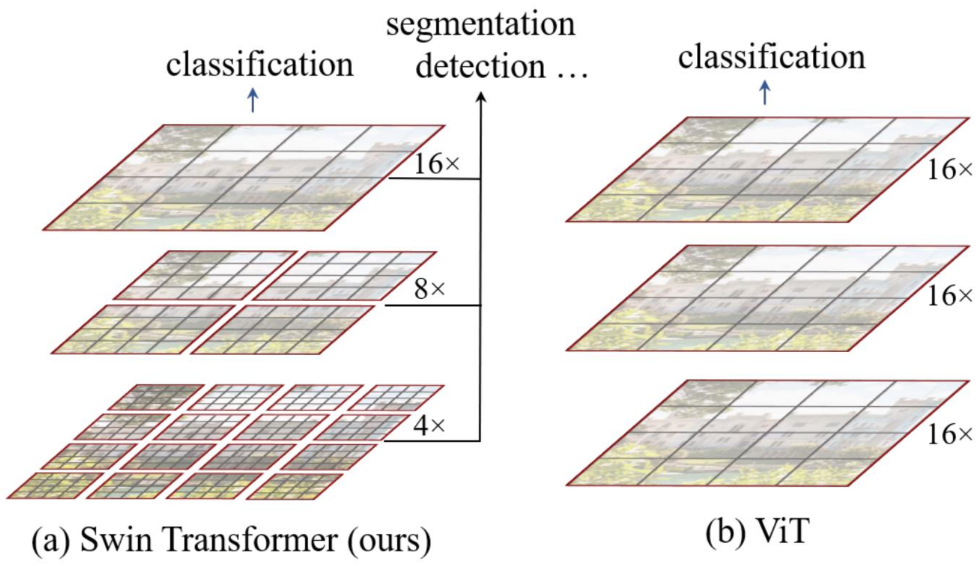

Architectures of Swin Transformer and Vision Transformer.

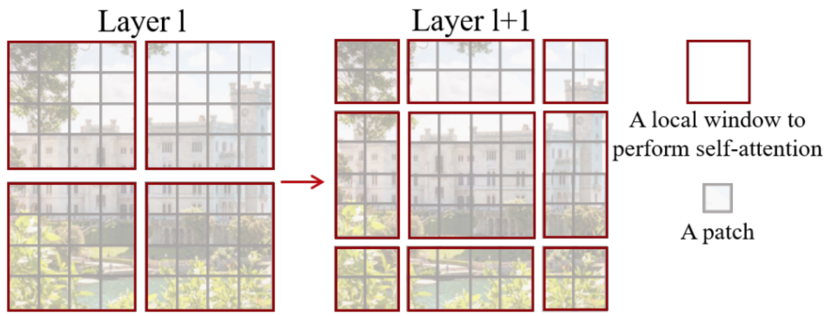

Figure 2. An illustration of the *shifted window* approach for computing self-attention in the proposed Swin Transformer architecture. In layer l (left), a regular window partitioning scheme is adopted, and self-attention is computed within each window. In the next layer $l+1$ (right), the window partitioning is shifted, resulting in new windows. The self-attention computation in the new windows crosses the boundaries of the previous windows in layer l, providing connections among them.

Swin Transformer

- Two successive Swin Transformer Block.

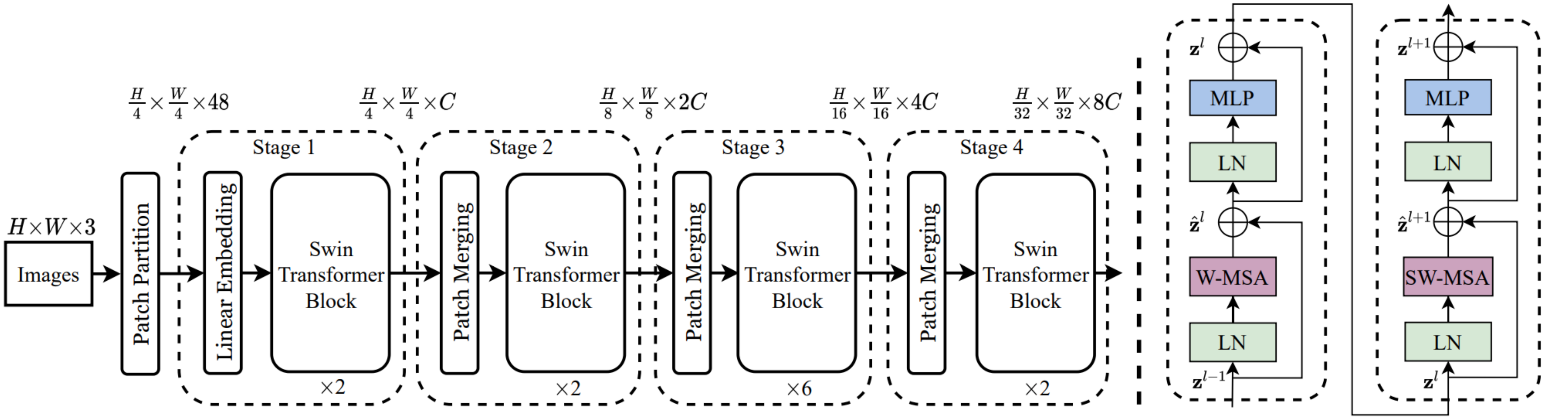

(a) Architecture (b) Two Successive Swin Transformer Blocks

Figure 3. (a) The architecture of a Swin Transformer (Swin-T); (b) two successive Swin Transformer Blocks (notation presented with Eq. (3)). W-MSA and SW-MSA are multi-head self attention modules with regular and shifted windowing configurations, respectively.

Efficient Batch Computation

- The number of batched windows remains the same as that of regular window partitioning.

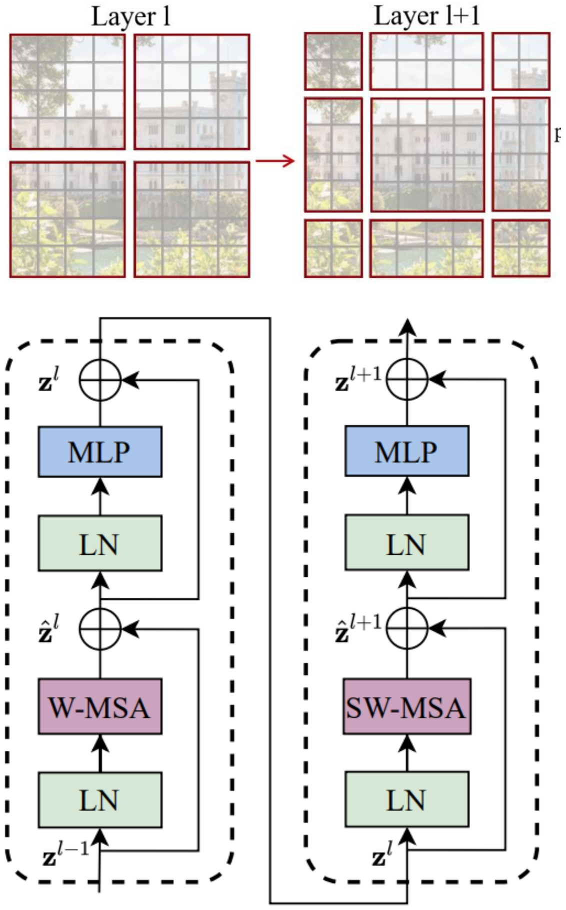

Two successive Swin Transformer Block.

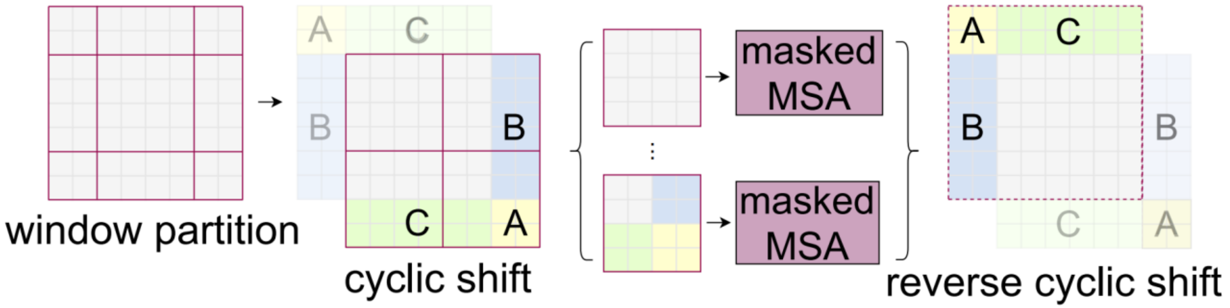

Figure 4. Illustration of an efficient batch computation approach for self-attention in shifted window partitioning.

method	MSA in a stage (ms) S1	S2	S3	S4	Arch. (FPS) T	S	B
sliding window (naive)	122.5	38.3	12.1	7.6	183	109	77
sliding window (kernel)	7.6	4.7	2.7	1.8	488	283	187
Performer [14]	4.8	2.8	1.8	1.5	638	370	241
window (w/o shifting)	2.8	1.7	1.2	0.9	770	444	280
shifted window (padding)	3.3	2.3	1.9	2.2	670	371	236
shifted window (cyclic)	3.0	1.9	1.3	1.0	755	437	278

Table 5. Real speed of different self-attention computation methods and implementations on a V100 GPU.

Relative Positional Bias

- Positional biases: absolute, relative
- Relative Positional Bias: $$\text{Attention}(Q, K, V) = \text{SoftMax}(QK^T/\sqrt{d} + B)V, \quad (4)$$
- A different window size through bi-cubic interpolation.

	ImageNet		COCO		ADE20k
	top-1	top-5	AP^{box}	AP^{mask}	mIoU
w/o shifting	80.2	95.1	47.7	41.5	43.3
shifted windows	**81.3**	**95.6**	**50.5**	**43.7**	**46.1**
no pos.	80.1	94.9	49.2	42.6	43.8
abs. pos.	80.5	95.2	49.0	42.4	43.2
abs.+rel. pos.	81.3	95.6	50.2	43.4	44.0
rel. pos. w/o app.	79.3	94.7	48.2	41.9	44.1
rel. pos.	**81.3**	**95.6**	**50.5**	**43.7**	**46.1**

Ablation studies of Swin and different positional biases

Architecture Variants

- Swin-T, Swin-S, Swin-B, Swin-L: 0.25×, 0.5×, 1×, and 2× the model size and computational complexity, respectively.

- **Swin-T**: $C = 96$, layer numbers = $\{2, 2, 6, 2\}$
- **Swin-S**: $C = 96$, layer numbers =$\{2, 2, 18, 2\}$
- **Swin-B**: $C = 128$, layer numbers =$\{2, 2, 18, 2\}$
- **Swin-L**: $C = 192$, layer numbers =$\{2, 2, 18, 2\}$

layer name	output size	18-layer	34-layer	50-layer	101-layer	152-layer
conv1	112×112	7×7, 64, stride 2				
conv2_x	56×56	3×3 max pool, stride 2				
		$\begin{bmatrix}3\times3, 64\\3\times3, 64\end{bmatrix}\times2$	$\begin{bmatrix}3\times3, 64\\3\times3, 64\end{bmatrix}\times3$	$\begin{bmatrix}1\times1, 64\\3\times3, 64\\1\times1, 256\end{bmatrix}\times3$	$\begin{bmatrix}1\times1, 64\\3\times3, 64\\1\times1, 256\end{bmatrix}\times3$	$\begin{bmatrix}1\times1, 64\\3\times3, 64\\1\times1, 256\end{bmatrix}\times3$
conv3_x	28×28	$\begin{bmatrix}3\times3, 128\\3\times3, 128\end{bmatrix}\times2$	$\begin{bmatrix}3\times3, 128\\3\times3, 128\end{bmatrix}\times4$	$\begin{bmatrix}1\times1, 128\\3\times3, 128\\1\times1, 512\end{bmatrix}\times4$	$\begin{bmatrix}1\times1, 128\\3\times3, 128\\1\times1, 512\end{bmatrix}\times4$	$\begin{bmatrix}1\times1, 128\\3\times3, 128\\1\times1, 512\end{bmatrix}\times8$
conv4_x	14×14	$\begin{bmatrix}3\times3, 256\\3\times3, 256\end{bmatrix}\times2$	$\begin{bmatrix}3\times3, 256\\3\times3, 256\end{bmatrix}\times6$	$\begin{bmatrix}1\times1, 256\\3\times3, 256\\1\times1, 1024\end{bmatrix}\times6$	$\begin{bmatrix}1\times1, 256\\3\times3, 256\\1\times1, 1024\end{bmatrix}\times23$	$\begin{bmatrix}1\times1, 256\\3\times3, 256\\1\times1, 1024\end{bmatrix}\times36$
conv5_x	7×7	$\begin{bmatrix}3\times3, 512\\3\times3, 512\end{bmatrix}\times2$	$\begin{bmatrix}3\times3, 512\\3\times3, 512\end{bmatrix}\times3$	$\begin{bmatrix}1\times1, 512\\3\times3, 512\\1\times1, 2048\end{bmatrix}\times3$	$\begin{bmatrix}1\times1, 512\\3\times3, 512\\1\times1, 2048\end{bmatrix}\times3$	$\begin{bmatrix}1\times1, 512\\3\times3, 512\\1\times1, 2048\end{bmatrix}\times3$
	1×1	average pool, 1000-d fc, softmax				
FLOPs		1.8×10^9	3.6×10^9	3.8×10^9	7.6×10^9	11.3×10^9

ResNet Architectures for ImageNet.

He, Kaiming, et al. "Deep residual learning for image recognition." *Proceedings of the IEEE conference on computer vision and pattern recognition*. 2016.

Quantitative Results

(a) Regular ImageNet-1K trained models

method	image size	#param.	FLOPs	throughput (image / s)	ImageNet top-1 acc.
RegNetY-4G [48]	224^2	21M	4.0G	1156.7	80.0
RegNetY-8G [48]	224^2	39M	8.0G	591.6	81.7
RegNetY-16G [48]	224^2	84M	16.0G	334.7	82.9
EffNet-B3 [58]	300^2	12M	1.8G	732.1	81.6
EffNet-B4 [58]	380^2	19M	4.2G	349.4	82.9
EffNet-B5 [58]	456^2	30M	9.9G	169.1	83.6
EffNet-B6 [58]	528^2	43M	19.0G	96.9	84.0
EffNet-B7 [58]	600^2	66M	37.0G	55.1	84.3
ViT-B/16 [20]	384^2	86M	55.4G	85.9	77.9
ViT-L/16 [20]	384^2	307M	190.7G	27.3	76.5
DeiT-S [63]	224^2	22M	4.6G	940.4	79.8
DeiT-B [63]	224^2	86M	17.5G	292.3	81.8
DeiT-B [63]	384^2	86M	55.4G	85.9	83.1
Swin-T	224^2	29M	4.5G	755.2	81.3
Swin-S	224^2	50M	8.7G	436.9	83.0
Swin-B	224^2	88M	15.4G	278.1	83.5
Swin-B	384^2	88M	47.0G	84.7	84.5

(b) ImageNet-22K pre-trained models

method	image size	#param.	FLOPs	throughput (image / s)	ImageNet top-1 acc.
R-101x3 [38]	384^2	388M	204.6G	-	84.4
R-152x4 [38]	480^2	937M	840.5G	-	85.4
ViT-B/16 [20]	384^2	86M	55.4G	85.9	84.0
ViT-L/16 [20]	384^2	307M	190.7G	27.3	85.2
Swin-B	224^2	88M	15.4G	278.1	85.2
Swin-B	384^2	88M	47.0G	84.7	86.4
Swin-L	384^2	197M	103.9G	42.1	87.3

Table 1. Comparison of different backbones on ImageNet-1K classification. Throughput is measured using the GitHub repository of [68] and a V100 GPU, following [63].

Quantitative Results

(a) Various frameworks

Method	Backbone	AP^{box}	AP^{box}_{50}	AP^{box}_{75}	#param.	FLOPs	FPS
Cascade Mask R-CNN	R-50	46.3	64.3	50.5	82M	739G	18.0
	Swin-T	**50.5**	**69.3**	**54.9**	86M	745G	15.3
ATSS	R-50	43.5	61.9	47.0	32M	205G	28.3
	Swin-T	**47.2**	**66.5**	**51.3**	36M	215G	22.3
RepPointsV2	R-50	46.5	64.6	50.3	42M	274G	13.6
	Swin-T	**50.0**	**68.5**	**54.2**	45M	283G	12.0
Sparse R-CNN	R-50	44.5	63.4	48.2	106M	166G	21.0
	Swin-T	**47.9**	**67.3**	**52.3**	110M	172G	18.4

(b) Various backbones w. Cascade Mask R-CNN

	AP^{box}	AP^{box}_{50}	AP^{box}_{75}	AP^{mask}	AP^{mask}_{50}	AP^{mask}_{75}	param	FLOPs	FPS
DeiT-S†	48.0	67.2	51.7	41.4	64.2	44.3	80M	889G	10.4
R50	46.3	64.3	50.5	40.1	61.7	43.4	82M	739G	18.0
Swin-T	**50.5**	**69.3**	**54.9**	**43.7**	**66.6**	**47.1**	86M	745G	15.3
X101-32	48.1	66.5	52.4	41.6	63.9	45.2	101M	819G	12.8
Swin-S	**51.8**	**70.4**	**56.3**	**44.7**	**67.9**	**48.5**	107M	838G	12.0
X101-64	48.3	66.4	52.3	41.7	64.0	45.1	140M	972G	10.4
Swin-B	**51.9**	**70.9**	**56.5**	**45.0**	**68.4**	**48.7**	145M	982G	11.6

(c) System-level Comparison

Method	mini-val		test-dev		#param.	FLOPs
	AP^{box}	AP^{mask}	AP^{box}	AP^{mask}		
RepPointsV2* [12]	-	-	52.1	-	-	-
GCNet* [7]	51.8	44.7	52.3	45.4	-	1041G
RelationNet++* [13]	-	-	52.7	-	-	-
SpineNet-190 [21]	52.6	-	52.8	-	164M	1885G
ResNeSt-200* [78]	52.5	-	53.3	47.1	-	-
EfficientDet-D7 [59]	54.4	-	55.1	-	77M	410G
DetectoRS* [46]	-	-	55.7	48.5	-	-
YOLOv4 P7* [4]	-	-	55.8	-	-	-
Copy-paste [26]	55.9	47.2	56.0	47.4	185M	1440G
X101-64 (HTC++)	52.3	46.0	-	-	155M	1033G
Swin-B (HTC++)	56.4	49.1	-	-	160M	1043G
Swin-L (HTC++)	57.1	49.5	57.7	50.2	284M	1470G
Swin-L (HTC++)*	**58.0**	**50.4**	**58.7**	**51.1**	284M	-

Table 2. Results on COCO object detection and instance segmentation. †denotes that additional decovolution layers are used to produce hierarchical feature maps. * indicates multi-scale testing.

Quantitative Results

ADE20K Method	Backbone	val mIoU	test score	#param.	FLOPs	FPS
DANet [23]	ResNet-101	45.2	-	69M	1119G	15.2
DLab.v3+ [11]	ResNet-101	44.1	-	63M	1021G	16.0
ACNet [24]	ResNet-101	45.9	38.5	-		
DNL [71]	ResNet-101	46.0	56.2	69M	1249G	14.8
OCRNet [73]	ResNet-101	45.3	56.0	56M	923G	19.3
UperNet [69]	ResNet-101	44.9	-	86M	1029G	20.1
OCRNet [73]	HRNet-w48	45.7	-	71M	664G	12.5
DLab.v3+ [11]	ResNeSt-101	46.9	55.1	66M	1051G	11.9
DLab.v3+ [11]	ResNeSt-200	48.4	-	88M	1381G	8.1
SETR [81]	T-Large‡	50.3	61.7	308M	-	-
UperNet	DeiT-S†	44.0	-	52M	1099G	16.2
UperNet	Swin-T	46.1	-	60M	945G	18.5
UperNet	Swin-S	49.3	-	81M	1038G	15.2
UperNet	Swin-B‡	51.6	-	121M	1841G	8.7
UperNet	Swin-L‡	**53.5**	**62.8**	234M	3230G	6.2

Table 3. Results of semantic segmentation on the ADE20K val and test set. † indicates additional deconvolution layers are used to produce hierarchical feature maps. ‡ indicates that the model is pre-trained on ImageNet-22K.

Paperswithcode

- https://paperswithcode.com/task/object-detection
- https://paperswithcode.com/task/semantic-segmentation